Pulse compression by stimulated Brillouin scattering

David T. Hon

Hughes Research Laboratories, Malibu, California 92065

Received August 25, 1980

A 20-nsec Nd:YAG laser pulse is compressed to a 2-nsec phase-conjugated pulse in a tapered glass tube filled with methane at 130 atm. A comparison with stimulated-Raman-scattering pulse compression is made. A semiclassical theory is proposed that agrees well with experimental results.

Pulse compression by backward-stimulated *Raman* scattering (SRS) has been studied quite thoroughly in recent years.[1-10] The possibility of pulse compression by stimulated *Brillouin* scattering (SBS) has also been noted,[2] especially in spurious damages occurring in long optical fibers.[11-15] We have recently demonstrated controlled pulse compression by SBS with high energy efficiencies.[16] The compressed pulse is wave-front reversed[17] (spatially phase conjugated) while the polarization state behaves like a mirror reflection. These facts combine to make this technique potentially extremely useful for compressing laser pulses to the 1-nsec regime.

In our experiment, a 200-mJ, 20-nsec pulse from a single-longitudinal-mode Nd:YAG laser is directed into a glass tube placed inside a methane (CH_4) cell pressurized to 130 atm. The inner diameter of the 1.3-m glass tube tapers gradually from 4 to 2 mm. By using a fast photodiode and a scope with a bandwidth of 500 MHz, the SBS pulse is measured to have a sharp leading spike of 2 ± 0.5 nsec, followed by a smooth tail that resembles the trailing half of the input pulse. This is shown as SBS1 in Fig. 1. This partially compressed, phase-conjugated pulse is allowed to return to the laser, where a second pulse (input 2) is generated. This pulse is compressed a second time by the same tapered tube to obtain a 2 ± 0.5 nsec pulse (SBS2). Also shown in Fig. 1 (shaded) is the energy transmitted during the first compression. After initially following the shape of input 1, the energy suddenly drops to zero, indicating a sudden transformation into full SBS conversion. We have estimated that 70% energy conversion is achieved in the first compression. As illustrated, input 2 has a very irreproducibly jagged shape that is characteristic of a multilongitudinal-mode pulse. This is probably because it results from an injected pulse (SBS1) whose Brillouin-shifted frequency does not match any longitudinal modes of the laser cavity. The short coherence length that input 2 has is probably responsible for the low energy efficiency of the second SBS compression. If desired, the backward-traveling SBS1 can be extracted easily and completely by the use of a polarizer and a 45°-oriented $\lambda/4$ plate.

In order to understand these compression results, it is appropriate first to compare SBS with the more familiar SRS. SRS is stimulated scattering from optical phonons, whereas SBS is from acoustic phonons. Several important differences are summarized in Table 1 for a typical liquid in the visible regime.[2]

In the theoretical treatment, the equations of motion of SRS are simpler than those of SBS because optical phonons are localized excitations in a fluid, whereas acoustic phonons are cooperative excitations. More importantly, the extremely small τ in SRS can often be ignored; this reduces the four equations of motion for backward SRS to the following form[1,2]:

$$-\frac{\partial I_s}{\partial z}+\frac{n}{c}\frac{\partial I_s}{\partial t}=\sigma I_s I_L,$$
$$\frac{\partial I_L}{\partial z}+\frac{n}{c}\frac{\partial I_L}{\partial t}=\sigma I_s I_L, \qquad (1)$$

where I_L is the input laser intensity, I_s is the backward SRS intensity, and σ is the coupling constant for light propagating along the z axis. In Eq. (1), n is the refractive index and c is the speed of light in a vacuum. Note that the phonon variable has been eliminated. Equation (1) is a basis for some common transient- and steady-state theories of SRS. SRS pulse compression and SRS amplifiers in general are quite well understood. A more elaborate theory explains why picosecond pulses—comparable with τ—have been achieved by SRS pulse compression.[1,18,19] (However, the fact that many SRS's are initiated by self-focusing, which is erratic, has made a full test of these theories a bit difficult.)

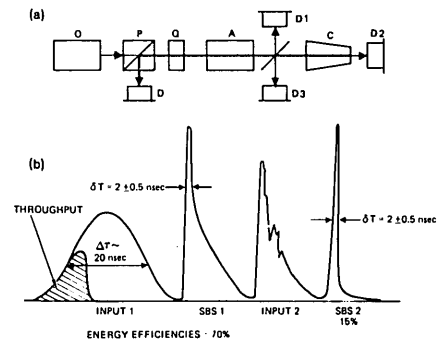

Fig. 1. (a) Schematic of experiment: O, oscillator; P, polarizer; Q, $\lambda/4$ plate; A, amplifier; C, SBS cell; and D's, detectors. (b) Input, throughput, and SBS signals as detected by D1, D2, and D3, respectively, in a two-step pulse compression.

0146-9592/80/120516-03$0.50/0

Table 1. Comparison between SRS and SBS for a Typical Liquid in the Visible Regime

	Relaxation Time τ (sec)	Frequency Shift (cm^{-1})	Cross Section (cm^{-1} sr^{-1})
SRS	10^{-12}	1000	10^{-7}
SBS	10^{-9}	1	10^{-6}

In contrast, transient SBS is much less well understood, even though the steady-state theory has been satisfactorily developed.

Ignoring temperature effects, the Navier–Stokes equation may be written as[2]:

$$-\frac{\partial^2\rho'}{\partial t^2}+v^2\Delta\rho'+\frac{\eta}{\rho_0}\frac{\partial\Delta\rho'}{\partial t}=\frac{\gamma^e}{8\pi}\Delta(E')^2, \tag{2}$$

where ρ' is the fluctuation of the medium's density from its average value ρ_0, v is the velocity of sound, η is the viscosity of the medium, and γ^e is the electrostrictive coupling constant. $E'=E_L'+E_S'$ is the total electric field arising from a plane incident wave E_L' traveling to the right and its SBS wave E_S' traveling in the opposite direction. Fortunately, it can be shown that, in the envelope approximation, where

$$\rho'=\frac{1}{2}\{\rho\exp[i(kz-\omega t)]+\text{c.c.}\}\text{ etc.},$$

all the spatial terms in the ensuing equation are negligibly small. We are left with

$$\frac{\partial^2\rho}{\partial t^2}-i\omega\left(2\frac{\partial\rho}{\partial t}+\Gamma\rho\right)=\frac{\gamma^e k^2}{8\pi}E_L E_S^*. \tag{3}$$

Equations (3,) (4), and (5) (Ref. 2) constitute the dynamic equations of SBS:

$$-\frac{\partial E_L}{\partial z}+\frac{n\partial E_s}{c\ \partial t}=\frac{i\omega_s}{4cn}\frac{\gamma^e}{\rho_0}E_L\rho^*, \tag{4}$$

$$\frac{\partial E_L}{\partial z}+\frac{n\partial E_L}{c\ \partial t}=\frac{i\omega_L\gamma^e}{4cn\rho_0}E_s\rho. \tag{5}$$

Here $\Gamma=\tau^{-1}=nk^2/\rho_0$ is the Brillouin linewidth. If the compressed pulse width δt is greater than τ, then only the ρ term in Eq. (3) is important, and Eqs. (3)–(5) can be reduced to the format of Eq. (1); then SRS pulse compression theory is applicable except for changes in constants. If δt is comparable with τ, the $\partial\rho/\partial t$ term at first tends to slow down the speed of compression but eventually can serve to compress the pulse further to the regime of $\delta t<\tau$, as in our experiment. In this regime, while the $\partial\rho/\partial t$ term compresses, the $\partial^2\rho/\partial t^2$ term will mathematically limit the pulse width to ω^{-1}. A full discussion of the dynamics of SBS pulse compression will be the subject of a future paper. For the moment, a simple semiclassical theory is presented that offers an intuitive picture of SBS pulse compression while providing results in good agreement with experiments.

The key to SBS compression is the tapered light guide. The threshold of SBS is reached by the leading edge of the pulse at the far end where the smaller diameter forces an increase of power density. As the SBS pulse sweeps backward, it beats with the remainder of the incident wave to create a strong acoustic wave with

$$k_0\sim 2k_L,\qquad \omega_0\sim 2nv_0\omega_L/c, \tag{6}$$

which in turn acts as a bulk grating to reflect the incident wave further to strengthen the SBS wave coherently[22]—all in accordance with Eqs. (3)–(5). Even though the phonon wave travels in the forward direction at a phase velocity of $\sim 10^5$ cm/sec, its amplitude envelope ρ must necessarily expand itself rapidly backward, following closely the leading edge of the SBS wave, which travels with a speed of c/n. It is postulated that the leading edge of this phonon envelope forms the mirror that reflects and, owing to its growing reflectivity, compresses the pulse. This is illustrated in the time sequence in Fig. 2. Such a postulate necessarily leads to the following quantitative model.

The reflectivity r of an acoustic wave, when the Bragg condition is satisfied as in the case here, is given by[23]:

$$r=\tanh^2(\pi l\sqrt{M_2I_0}/\sqrt{2}\lambda), \tag{7}$$

where l is the interaction depth, I_0 is the acoustic power density, and

$$M_2=n^6P_{12}^2/\rho_0v_0^3, \tag{8}$$

the acousto-optic figure of merit, with p_{12} the elasto-optic constant. It can easily be shown that within 5%, Eq. (7) can be approximated by a simpler equation,

$$r\sim\sin^2(\pi l\sqrt{M_2I_0}/2\lambda). \tag{9}$$

To calculate I_0, let us assume a square incident pulse in a uniform light guide of diameter d. Let us assume that there exists an interaction region with length L, in which efficient SBS occurs. This is suggested by the transmitted pulse shape in Fig. 1. Since the creation of one SBS photon entails the creation of one phonon, the following is true:

$$(dN_s/dt)=(dN_0/dt), \tag{10}$$

where N_s and N_0 are the total number of SBS photons and phonons, respectively, produced in this interaction volume during a photon round-trip time of

$$T=2nL/c. \tag{11}$$

If we further assume zero attenuation, then the following will be true:

$$N_s=N_0. \tag{12}$$

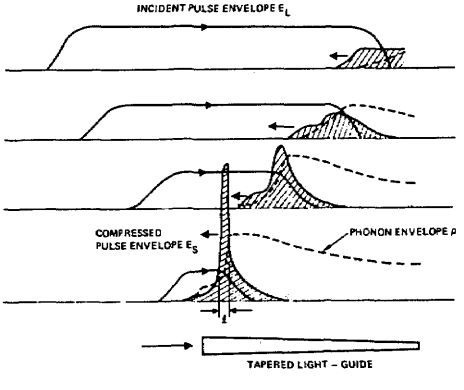

Fig. 2. Time sequence of SBS compression of a square incident pulse in a tapered light guide.

This assumption is not unreasonable for our experiment, in which the cell length is 1.3 m, so T is at most 8 nsec while the phonon lifetime is about 30 nsec.

Thus the acoustic energy $\mathcal{E}_0$ produced is

$$\mathcal{E}_0 = N_0\hbar\omega_0 = (\mathcal{E}_L r'\omega_0/\omega_s), \tag{13}$$

where r' is the SBS efficiency and $\mathcal{E}_L$ is the incident energy encountered by the leading edge of the backward SBS wave in time T within the volume $L \times d^2$. The acoustic power density is

$$I_0 \sim \mathcal{E}_0 v_0/Ld^2 \sim r'\mathcal{E}_L\omega_0 v_0/Ld^2\omega_L. \tag{14}$$

Substituting Eqs. (6), (8), and (14) into Eq. (9), and setting $r = r' = 1$, one obtains

$$l \sim (\lambda c/2n^4 p_{12})\sqrt{\rho_0 v_0/P}, \tag{15}$$

where $P = (\mathcal{E}_L/Td^2) = (c\mathcal{E}_L/2nLd^2)$ is the power density of the incident light. Now l is the *penetration depth* of the acoustic wave necessarily generated in an efficient SBS. If it is not larger than L, it may be considered as the thickness of the bulk-grating mirror, which is the leading edge of the phonon envelope, that sweeps backward at the speed of c/n. The incident energy is being swept up and turned around within a region of space that is l long. The compressed pulse width is therefore simply

$$\delta T \sim nl/c \sim (\lambda/2n^3 p_{12})\sqrt{\rho_0 v_0/P}. \tag{16}$$

For CH_4 at 130 atm, on calculating p_{12} with the help of Refs. 12 and 21, we find that $\delta T = 2.1$ nsec. (In Ref. 12, the SBS gain is given by $g = 2\pi n^7 p_{12}/c\lambda^2\rho_0 v_0\Delta\nu$. In Ref. 21, $g \sim 0.09$ cm/MW and $\Delta\nu \sim 20$ MHz are measured.) It is perhaps fortuitous that the result from such a model agrees so well with the observed values of 2 ± 0.5 nsec. But it must be stressed that the assumption of zero attenuation leading to Eq. (12) is more justified now because $\delta T \ll \tau \sim 30$ nsec. Only fresh phonons at the leading edge of the envelope play any role in the reflectivity.

Of course, Eq. (16) is true only if the conditions leading up to it are satisfied. Our experimental setup satisfies these conditions with perhaps one flaw, namely, that the cell is only 1.3 m long. Ideally it should be about half of the pulse length, or 3–4 m, if one wishes to compress a 20-nsec pulse in one passage. As it is, about half of the energy is compressed into one spike of 2 nsec. The strong acoustic wave left in the pulse's wake (remember that damping time $\tau \sim 30$ nsec) then effectively backscatters the remainder of the pulse near the entrance end by the inertial property familiar in double-pulse SBS experiments.[20] This shows itself as the tail of SBS1 in Fig. 1.

Significantly, Eq. (16) is independent of L. In fact, for an incident pulse of uniform power density, it describes the constant width of a leading spike, which, if given a chance, will grow to great magnitudes to dominate the entire SBS pulse. It is almost certain that SBS pulse compression is responsible for the damage of many optical fibers.[11–15]

From Eq. (16), the peak power density P_c of the compressed pulse is given by

$$P_c \sim (2n\Lambda P/c\delta T) \sim (4\Lambda n^4 p_{12} p^{3/2}/c\lambda\sqrt{\rho_0 v_0}), \tag{17}$$

where Λ is the length of an effective compressor cell suitable to compress a square pulse of width $\Delta T = (2n\Lambda/c)$ or to compress a cw laser into a train of pulses with periodicity ΔT. If peak power damage is (naively) taken as a limiting mechanism for SBS pulse compression, Eqs. (16) and (17) can be reformulated to give

$$(\delta T)_M \sim (\Lambda\lambda^2\rho_0 v_0/2cP_m n^5 p_{12})^{1/3}, \tag{18}$$

where $(\delta T)_M$ is the minimum pulse width achievable in a medium with a peak-power-damage threshold of P_M. Because of the cubed root in Eq. (18), $(\delta T)_M$ should be relatively insensitive to specific material parameters and should fall within the 0.2–2-nsec range.

Other potential limiting mechanisms that may limit SBS pulse compressions are forward SRS and self-focusing. These can be solved by using Raman-weak materials and by proper use of guided geometry, respectively.

Finally, no multiple SBS is detected. This is not surprising because $\delta T \ll \tau$. Thus the slower response of SBS is an important advantage in pulse compression over SRS, whose fast τ consistently lead to multiple scattering in experiments designed for power scaling.

I thank A. Yariv, R. W. Hellwarth, and D. M. Henderson for useful discussions.

References

1. M. Maier *et al.*, Phys. Rev. 177, 580 (1969).
2. W. Kaiser and M. Maier, in *Laser Handbook* (North-Holland, Amsterdam, 1972), Vol. 2, p. 1078.
3. W. H. Lowdermilk and G. I. Kachen, J. Appl. Phys. **50,** 3871 (1979).
4. A. Penzkofer *et al.*, Prog. Quantum Electron. **6,** 55 (1979).
5. I. M. Beldyugin and E. M. Zemskov, Sov. J. Quantum Electron. **8,** 1163 (1978).
6. J. J. Ewing *et al.*, IEEE J. Quantum Electron. **QE-15,** 368 (1979).
7. J. R. Murray *et al.*, IEEE J. Quantum Electron. **QE-15,** 342 (1979).
8. V. N. Lugovoi and V. N. Streltsov, Sov. J. Quantum Electron. **6,** 971 (1976).
9. N. Tan-No *et al.*, Phys. Rev. A **12,** 159 (1975).
10. A. Z. Grasyuk *et al.*, Sov. J. Quantum Electron. **3,** 380 (1974).
11. R. G. Smith, Appl. Opt. **11,** 2489 (1972).
12. E. P. Ippen and R. H. Stolen, Appl. Phys. Lett. **21,** 539 (1972).
13. K. O. Hill *et al.*, Appl. Phys. Lett. **29,** 185 (1976).
14. G. D. Crow, Appl. Opt. **13,** 467 (1974).
15. P. Labudde *et al.*, Opt. Commun. **32,** 385 (1980).
16. D. T. Hon, presented at the Eleventh International Quantum Electronics Conference, Boston, Mass., 1980.
17. B. Y. Zeldovich *et al.*, JETP Lett. **15,** 109 (1972).
18. W. H. Culver *et al.*, Appl. Phys. Lett. **12,** 189 (1968).
19. A. J. Glass, IEEE J. Quantum Electron. **QE-3,** 516 (1967).
20. V. F. Efimkov *et al.*, Sov. Phys. JETP **50,** 267 (1979).
21. V. I. Kovalev *et al.*, Sov. J. Quantum Electron. **2,** 69 (1972).
22. J. Walder and C. L. Tang, Phys. Rev. Lett. **19,** 623 (1967).
23. See, for example, A. Yariv, *Quantum Electronics,* 2nd ed. (Wiley, New York, 1975), Secs. 14.9 and 19.5.